Bulletin de l'Institut royal du Patrimoine artistique / Bulletin van het Koninklijk Instituut voor het Kunstpatrimonium

40 | 2025
Varia

Post–Flood Recovery of Built Heritage: Modelling for Predicting Secondary Damage

José Vetro and Julie Desarnaud

Electronic version
URL: https://journals.openedition.org/kikirpa/7370
DOI: 10.4000/145tc
ISSN: 2983-855X

Publisher
Institut royal du Patrimoine artistique - Koninklijk Instituut voor het Kunstpatrimonium

Electronic reference
José Vetro and Julie Desarnaud, "Post–Flood Recovery of Built Heritage: Modelling for Predicting Secondary Damage", *Bulletin de l'Institut royal du Patrimoine artistique / Bulletin van het Koninklijk Instituut voor het Kunstpatrimonium* [Online], 40 | 2025, Online since 11 June 2025, connection on 19 June 2025. URL: http://journals.openedition.org/kikirpa/7370 ; DOI: https://doi.org/10.4000/145tc

Post–Flood Recovery of Built Heritage: Modelling for Predicting Secondary Damage

José Vetro and Julie Desarnaud

Introduction

Built heritage represents a non–renewable resource in terms of socio–cultural and economic uniqueness.[1] However, it remains fragile and highly vulnerable due to prolonged exposure to environmental factors, a vulnerability worsened by climate change. Climate change goes hand–in–hand with extreme weather events. The variability and severity of such events appear to be increasing in Europe, for instance, leading to droughts, floods, severe storms, and extensive heatwaves.

The risk management cycle following an extreme event, such as a flood, comprises three interconnected phases: 1) Emergency response, 2) Recovery, and 3) Disaster prevention and preparedness.[2] The emergency response phase centres on immediate stabilisation efforts that aim to save lives and minimise primary damage[3] (fig. 1). Following this is the recovery phase, during which the objectives are to implement measures that prevent secondary damage and restore the affected buildings.[4] Primary damages are evident damages and the direct consequences of the presence of water, such as staining. Secondary damage includes subsequent effects, like moisture spreading to areas initially unaffected by the water;[5] this can result in salt weathering or mould growth.

Finally, the last phase, disaster preparedness, encompasses both preventative measures and crisis management preparations. This entails planning for emergencies and developing strategies to protect cultural heritage during such crises.

In the summer of 2021, Belgium and parts of central Europe faced severe flooding due to heavy rainfall over one to two days. The situation was exacerbated by already saturated soil and local hydrological conditions.[6]

The water level reached between 1 and 2 metres inside buildings. In the Liège Province, 100 listed properties were affected, representing 10% of the province's heritage. Half of these properties are located in Verviers, where 60% of Verviers's heritage was impacted.[7]

[Fig. 1]

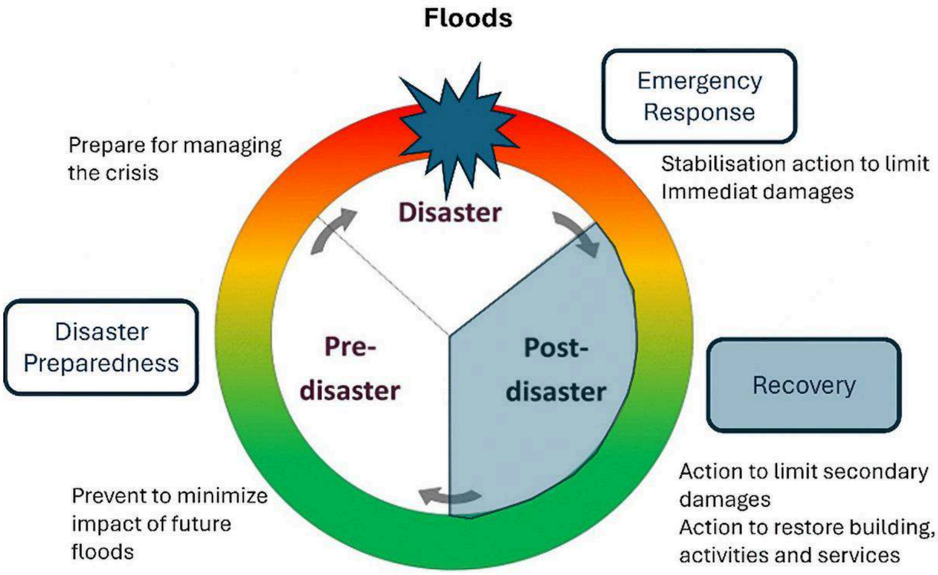

Risk Management Cycle – The actions described in this paper form part of the recovery phase (highlighted in blue), drawing inspiration from Pickels *et al.* 2015.

This paper focuses on the recovery phase of flood management, as it represents a crucial opportunity to address damages, improve the sustainability of the affected buildings, and strengthen community resilience.[8] Furthermore, it will emphasise the importance of considering the transition and interconnection between the response and recovery phases through long–term risk assessment.

Drawing on the flood management experience in Wallonia in 2021, this study aims to study the use of a thermodynamic ECOS/RUNSALT model to predict favourable conditions for salt damage and Sedlbauer's isopleths to predict the risk of mould growth. These predictions could aid site managers in prioritising recovery actions to mitigate secondary damage and implement the most suitable conservation treatments for flood–affected buildings.

Materials and Methodology

The primary cause of secondary damages is moisture, both within the building structures and as water vapour, which alters the indoor climate. Following damage documentation, emergency repair, and cleaning, the initial steps essential for an effective recovery process for built heritage affected by floods include monitoring and assessing moisture and salt content, identifying salts, monitoring climatic conditions (indoor and outdoor relative humidity and temperature), and monitoring mould growth.

As part of the CHrisis project, these parameters have been monitored and assessed in eight heritage buildings impacted by the 2021 floods in the province of Liège, Wallonia. The buildings encompass six churches, one residential dwelling, and one museum, all of which possess significant heritage value (fig. 2).

Different recovery approaches were carried out depending on the intensity and type of building degradation. The church Saint–Laurent of Trooz (fig. 2, red frame) presented the ideal situation for predicting mould growth and salt weathering.

[Fig. 2]

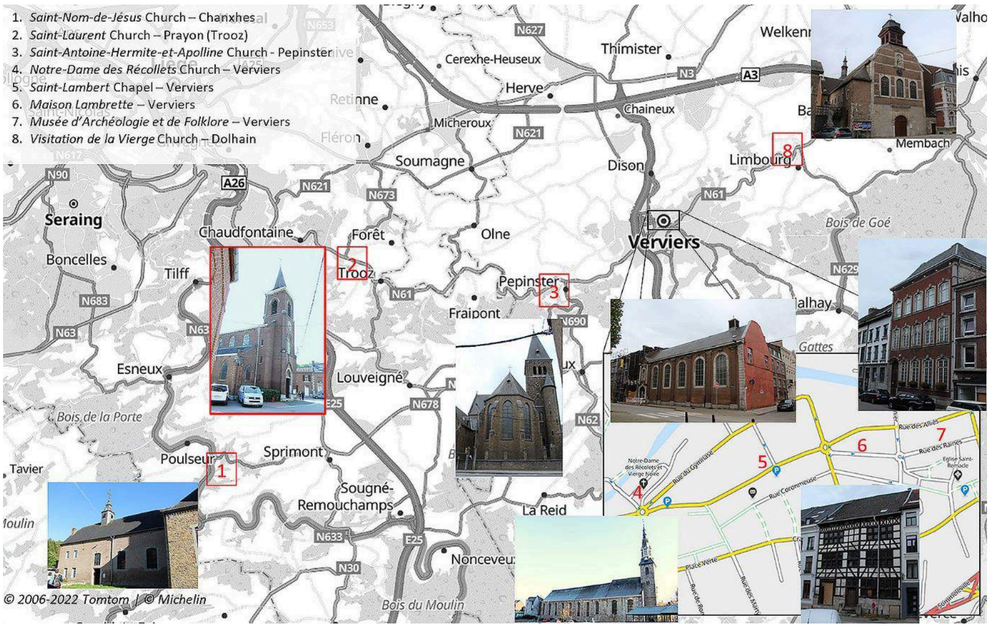

Photographs and locations of the heritage buildings studied in the CHrisis project (with Trooz Church in a red frame).

Monitoring Relative Humidity and Temperature

From April 2023 to April 2024, relative humidity (RH) and temperature (T) were measured continuously in the church of Trooz. Measurements were taken every hour and recorded by RH and T sensors throughout the year. The data was subsequently transmitted to a local LoRaWAN gateway situated in the church, which then sent it to a cloud–based IoT (Internet of Things) web platform. This platform provides live updates on relative humidity and temperature, both inside and outside the building.

Moisture, Hygroscopic Moisture and Ion Contents

The moisture content profiles in the building structures has been measured in order to determine the spatial moisture and salt content. The results presented here correspond to the measurements performed in February 2024.

Powder samples have been slowly drilled from building materials in the masonry (Bricks, plasters and mortar) at four different heights regarding ground level inside the church (20, 50, 100 and 150 cm) and two depths (0–5 and 5–10 cm). Profiles were taken from three walls (the external nave wall facing west, the external nave wall facing east, and the external wall of the choir facing north). For these samples, the moisture content (MC) was determined gravimetrically after drying at 60°C as follows:

$$MC\ (\%) = \frac{\left(weight_{wet} - weight_{dry}\right)}{weight\ _{dry}}.100$$

(1)

Samples are then placed in a climatic chamber with 95% relative humidity. After two weeks, the weights of the samples are measured again, and the hygroscopic moisture content (HMC) is calculated as follows:

$$HMC\ (\%) = \frac{\left(weight_{95\%} - weight_{dry}\right)}{weight\ _{dry}}.100$$

(2)

In this context, hygroscopic moisture is an indicator of the presence of hygroscopic salts. This measurement will be compared to the moisture content (MC) to ascertain the contribution of salt to the total water amount. A critical moisture content threshold of 3–5% in masonry has been established for MC; intervention is necessary if the moisture content exceeds this value. Conversely, if the moisture content falls below this threshold, no treatment is required.[9]

Identification of Salts and Determination of Crystallisation Behaviour

Subsequently, ultrapure water was added to the dried samples to extract the salts. This extract was analysed using ion chromatography (Metrohm) to quantify the amounts of Na^+, K^+, Mg^{2+}, Ca^{2+}, Cl^-, NO_3^-, and SO_4^{2-}. The ion analysis and data treatment are extensive and specific: the identification of salt mixtures and their behaviour under varying relative humidity (RH) conditions is based on the ion dataset corrected to achieve an equilibrium charge balance within each sample.[10] The balanced ion concentrations are presented as mole fractions, while the equimolar contents of calcium and sulphate, regarded as the gypsum content, are excluded. The data were used as direct input for the ECOS/RUNSALT model.[11] This model operates on principles analogous to the molality–based model, commonly known as the Pitzer–Simonson–Clegg model, which includes ion concentrations expressed as mole fractions.[12] The outputs of the model are investigated to determine the crystallisation behaviour of salt mixtures under changing RH between 15 and 95% with a 0.2% resolution at 15°C.

Mould Prediction Modelling and Mould Activity

In this study, the assessment of mould growth risk has been determined by modeling. As relative humidity (or water activity), temperature, and exposure time are the primary factors inducing mould, the relationship between these factors and mould risk is often illustrated using isopleth curves,[13] the Smith and Hill[14] model, and the ESP–r model developed by Hens,[15] which serve as the foundation for mould model development. These curves differentiate between favourable and unfavourable temperature and relative humidity conditions for mould growth. The simplest models just provide the limit state curve, more advanced isopleth models subdivide in time till germination and growth rate. The Sedlbauer isopleth model has been applied to predict mould growth risk.[16] He developed a lowest isopleth for mould (LIM), below which no mould will grow but also isopleths indicating the critical RH and temperature threshold to initiate mould spore germination for a specified time (e.g. 1, 2, 4... days). Furthermore, Sedlbauer developed LIM curves for various substrate categories. This study focuses on category II, which pertains to porous building materials such as renderings and mineral–based construction materials.[17]

The results of mould growth risk obtained through modelling have been compared with mould activity measured by ATP monitoring devices; ATP (adenosine triphosphate) is found in all living cells. Once the cells die, the ATP decays. The ATP test relies on the firefly luciferase reaction, which produces light from luciferin and ATP.[18] The amount of light generated is proportional to the quantity of ATP in a sample and can be quantified rapidly (within seconds) by measuring the light with a luminometer that displays the results in relative light units (RLU).[19] The presence of ATP thus serves as a marker for organic contamination on the tested surface. The measurement consists of three steps: 1) collecting the sample over three wall surfaces of 100 cm^2 with a disposal swab; 2) mixing the swab with luciferase reactant; 3) putting the solution (by–product from the reaction) in a luminometer and measuring the amount of photons (light). A consistent swab protocol adapted from manufacturers[20] has been established to enhance the reliability of measurements taken with an ATP SystemSure® device. The RLU values indicative of contamination can be categorised:[21]

From 0 RLU to 30 RLU: no living cells are present

From 30 RLU to 250 RLU: dormant spores

From 250 RLU to 500 RLU: active sporulation and growth

Beyond 500 RLU: high level of growth

This study deduces only the presence of active mould from the ATP test results.

Results and Discussion

Mould Growth Prediction

Once the mud was cleaned from the entire church with water during the emergency response phase in August 2021, the church remained closed, with only one window open in the sacristy. In February 2023, significant mould contamination was observed on the indoor wall surface (fig. 3).

[Fig. 3]

Church of Trooz. a) A picture of the wall fifteen days after the floods in August 2021 and b) one and a half years after the floods in February 2023.

Figure 4 demonstrates that half of the measurements surpass Sedlbauer's LIM curve for mould spore germination (represented by the red line in the graph), indicating that the conditions within the church are favourable for mould growth, especially during winter. Mould development on the wall surfaces has been observed at the end of winter.

The mould germination graph method takes into account temperature and humidity over previous time intervals, allowing for the consideration of fluctuating factors (fig. 4). This is essential, as certain conditions only foster mould growth if sustained for a sufficient duration. According to Pasanen,[22] under fluctuating humidity conditions, mould germination does not occur outside a specific range of favourable conditions. Within this favourable range, a delay in the rate of mould growth is observed if germination has already begun.

Mould germination is assumed to fail if environmental conditions fall outside the optimal range for growth. In this case, the accumulated exposure time is set at 0.

[Fig. 4]

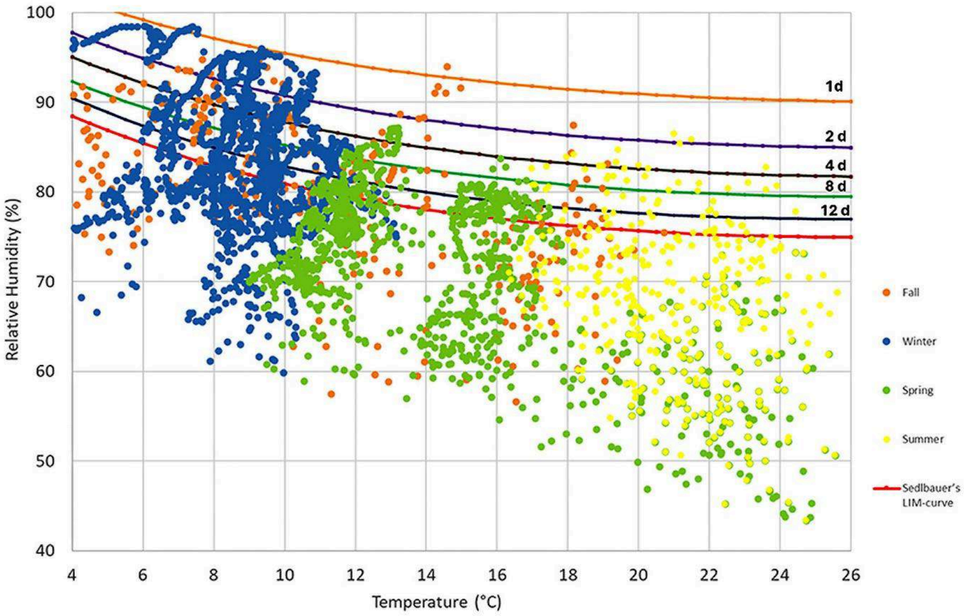

Relative humidity is measured every hour in the church's choir, along with Sedlbauer's isopleths for spore germination, as it relates to temperature.

This calculation has been conducted on the data (relative humidity and temperature near the surface) collected for the Church of Trooz. All data above the Sedlbauer curve–LIM have been selected. After this step, the accumulated exposure time can be calculated. An accumulated exposure time that is greater than or equal to the required exposure time indicates a risk of mould growth. The results, as illustrated in figure 5, highlight 22 periods classified as 'at risk'; however, when compared to the mould germination graph method, taking into account the required exposure time, only 7 of these periods can be considered to pose a significant risk for mould growth (highlighted in red).

[Fig. 5]

Period	Air Close to the surface		Accumulated exposure (days)	Required exposure time (days)	Mould growth risk	RLU
	T°C	RH %				
1	15.9	77.9	25.25	16	x	1200
2	19.1	77.3	16.1	16	x	750
3	21.4	82.1	1	4	0	900
4	22.9	76.6	6	16	0	900
5	22.3	76.5	1.5	16	0	900
6	18.5	81.4	2.75	5	0	900
7	18.6	75.2	3.75	32	0	450
8	17.8	76.2	6.25	32	0	708
9	13.2	82.8	17	8	x	708
10	9.5	83.2	29	16	x	390
11	4.3	88.9	3.75	24	0	250
12	7.9	88.0	29	7	x	500
13	5.5	96.2	5	2	x	500
14	6.6	87.6	3.2	12	0	544
15	9.0	89.0	21	4	x	1870
16	8.0	82.8	1.4	32	0	2180
17	10.3	84.2	5.5	10	0	2182
18	11.4	80.5	3.1	30	0	2182
19	12.4	79.1	1.6	32	0	2182
20	11.3	79.3	1	30	0	2182
21	13.9	80.6	6.25	15	0	1338
22	15.8	77.5	2	30	0	1750

Risk assessment using Sedlbauer's isopleths for the spore germination system and RLU measurements (x: mould growth risk, 0: no mould growth risk).

Furthermore, figure 5 presents the monthly ATP measurements (RLU). The results reveal five active periods of sporulation and growth and 17 periods of high growth. There appears to be no clear correlation between the ATP test results and the mould growth risk derived from isopleths.

The difference between the ATP measurements and the risk prediction based on Sedlbauer's isopleths for spore germination can first be explained by the sampling. For ATP, sampling is conducted only once a month, which does not precisely correspond to the entire accumulation exposure time period.

Secondly, the relative humidity and temperature plotted in the Sedlbauer isopleths implemented in the model are the measured relative humidities and temperatures measured in the air close to the wall, not the surface conditions, while the RLU includes the conditions in the wall to a larger extent.

It is also noteworthy that mould growth was observed as early as February 2023, with a very fast development, two months prior to the beginning of relative humidity monitoring. This indicates that 'Period 1', identified as a risk period according to the Sedlbauer's isopleths for spore germination, corresponds to ATP measurements taken from surfaces where visible mould growth was present. As soon as germination has started according to the Sedlbauer's isopleths, it is assumed that mould growth can start. Even if later on there are some unfavourable conditions mould spores are still 'active' (germination has started, so mould growth can start); In this way, ATP measurement and Sedlbauer's isopleths concur.

In all cases, the data above the Sedlbauer curve–LIM I correspond to active sporulation and significant mould growth based on ATP results. This means that the humidity and temperature monitoring can be used with the Sedlbauer's curve–LIM I model to predict the risk of mould growth.

Consequently, site managers can utilise it to prioritise actions aimed at mitigating secondary damage during the recovery process following floods.

Moisture Content and Salt Crystallisation Behaviour Prediction

The measurement of moisture and hygroscopic moisture content by gravimetry allows for the determination of the water source in the wall. The results obtained are presented in figure 6. Humidity contents higher than 3% have been only found in the plaster and the joint mortar, the moisture content in the brick is very low because of its low capillarity. For the moisture profiles acquired from the two nave walls, one facing west (fig. 6a) and the other facing east (fig. 6b), the hygroscopic moisture content (HMC) surpasses the measured moisture content (MC). This suggests that the predominant source of moisture is the presence of hygroscopic components, such as salts. In the wall located in the choir area (fig. 6c), only three sampling heights were possible due to the presence of a marble skirting board. The MC is always higher than the HMC. The moisture content (MC) in this wall exhibits a gradient, being higher at lower elevations and decreasing with increased height. Salt concentrations remain generally low throughout the wall, except within the plaster layer, where notable salt accumulation occurs at approximately 100 cm and 150 cm. This suggests that rising damp is the principal water source.

[Fig. 6]

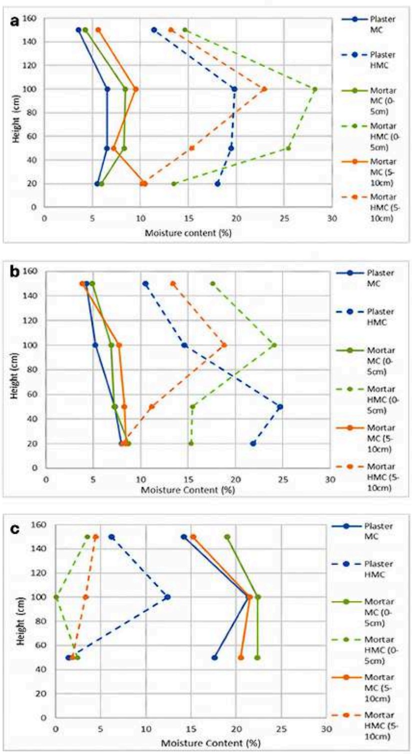

Moisture (MC) and hygroscopic moisture (HMC) content profiles: a) profile of the nave's west wall, b) profile of the east nave wall, and c) profile of the choir wall, measured in both the plaster and mortar at two depths: from 0 cm to 5 cm, and from 5 cm to 10 cm.

The total amount of ions determined by IC (Ion Chromatography) shows very low amount of salts in the wall of the choir but the nave's walls present high total amount of ions up to 100 cm (fig. 7). An high content of ions is only measured in the joint mortar and plaster. Consequently, salt weathering risk is only concentrated on these materials.

[Fig. 7]

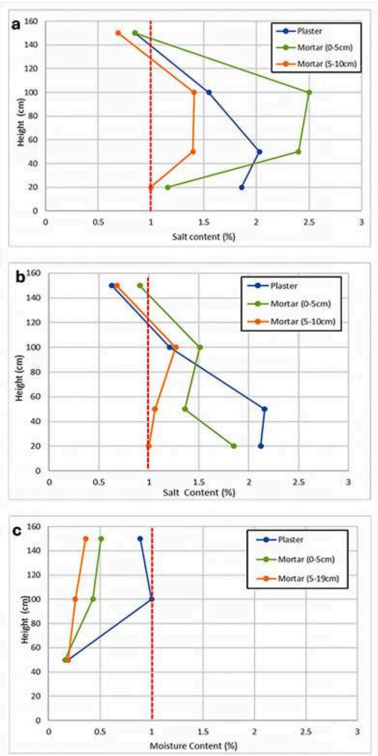

The salt content profiles of a) the nave's west wall, b) the east nave wall, and c) the choir wall.

The ECOS/RUNSALT models the crystallisation behaviour of a salt mixture from samples collected at the Trooz Church. The salt content exceeded 1% (after subtracting the equimolar content of sodium, calcium, and sulphate ions), which is regarded as a threshold above which treatment becomes essential to prevent future damage.

The results obtained of salt mixture crystallisation behaviour from the sampling of February 2024 are presented in table of figure 9 and annex 1. Figure 8 illustrates the results of ECOS/RUNSALT model output obtained for the sample taken from joint mortar in between 5–10 cm depth at a height of 50 cm in the west–facing wall. The salt mixture is mainly composed of niter (KNO_3) halite (NaCl) and bloedite (Na_2SO_4.$MgSO_4$.$4H_20$) and aphtitalite ((Na_2SO_4.$3K_2SO_4$). Their relative humidity of crystallisation in this mixture are 63% for niter, 68% for halite, 74% for bloedite, and 81% for the aphtitalite (with a resolution of 0.2%) at 15°C. Additionally, a small amount of aphtitalite, kieserite, and starkeite are present. The phase transitions of the main salts in this mixture occur between 63% and 81% RH. This means that in this RH interval dissolution and crystallisation cycles are likely to take place, making this range particularly susceptible to salt weathering processes (fig. 8).

[Fig. 8]

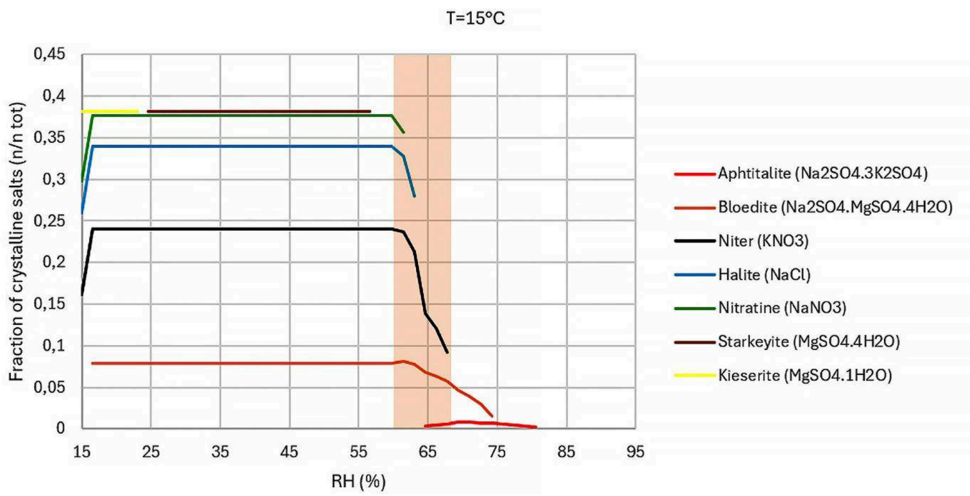

Crystallisation behaviour for varying relative humidity (15–95%) (0.2% resolution) (x–axis) at 20°C and 15°C of the ion mixture detected in a joint mortar sample (after subtracting an equimolar content of sodium, calcium, and sulphate ions) produced by the ECOS/RUNSALT model. The relative amount of substance is expressed as a fraction of crystalline salt (n/n_{tot}) (y–axis). The sample was collected from the surface of the joint mortar at 50 cm above ground level. The beige areas indicate the ranges of relative humidity that induce solid/liquid phase changes of the salts present in the sample. Mole fractions: Cl^-: 0.0988, NO_3^-: 0.1989, SO42–: 0.1625, Na+: 0.3063, K^+: 0.2951, K^+: 0.1611, and Mg^{2+}: 0.0833.

The common solids identified in the two walls of the nave are nitre (KNO_3), halite (NaCl), bloedite ($Na_2SO_4.MgSO_4.4H_2O$), and starkeyite ($MgSO_4.4H_2O$). Nitratine ($NaNO_3$) is found only in the wall facing west.

ECOS/RUNSALT has modelled the crystallisation behaviour of each salt mixture identified in the nave's walls (Appendix 1). Figure 9 illustrates the RH crystallisation intervals of the primary salts in mixtures with a total ion content exceeding 1% (excluding gypsum).

[Fig. 9]

15°C			RH crystallisation interval (%)		15°C			RH crystallisation interval (%)	
Localisation: West–facing wall					**Localisation: East–facing wall**				
Height (cm)	**Sample**	**Depth (cm)**			**Height (cm)**	**Sample**	**Depth (cm)**		
100	Mortar	5–10	60	66	150	Mortar	5–10	63	81
100	Mortar	0–5	60	68	100	Mortar	0–5	60	68
100	Plaster	–	57	68	100	Plaster		60	65
50	Mortar	5–10	60	81	50	Mortar	5–10	63	85

50	Mortar	0–5	57	74	50	Mortar	0–5	63	80
50	Plaster	–	57	74	50	Plaster		60	79
20	Mortar	0–5	57	81	20	Mortar	0–5	63	85
20	Plaster	–	57	75	20	Plaster		63	85

Relative humidity intervals at 15°C for the salt mixture were determined from samples taken in April 2024, which contained over 1% total ion content, while considering the heights, materials, depth of the investigated walls.

The phase transitions of the primary salts in the mixture, as determined in both walls, occur between 57% and 81% relative humidity. This indicates that, within this relative humidity range at 15°C, dissolution and crystallisation cycles may contribute to salt weathering.

The fluctuations in relative humidity (RH) monitored in the Church's nave area from April 2023 to April 2024 are illustrated in figure 10. Throughout the year, the air's RH displays significant variability, ranging from 52% to 100%. The humidity interval between 57% to 81% occurs frequently within the Trooz Church, particularly between April and October (indicated by the dashed lines in figure 10), highlighting a high risk of damage.

[Fig. 10]

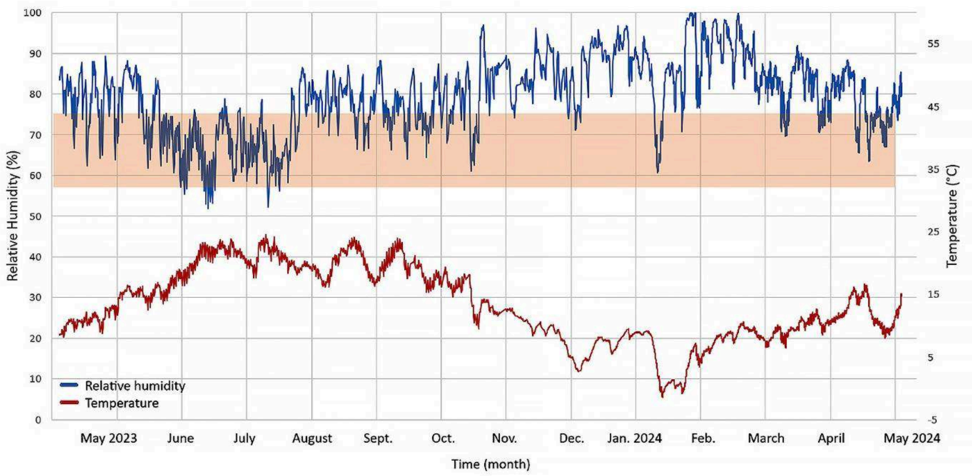

The graph illustrates fluctuations in relative humidity (blue) and temperature (red) within the nave of Trooz Church from 01 April 2023 to 30 April 2024. The beige zone denotes humidity fluctuations between 57% and 81% RH, which resulted in changes to the solid/liquid phase of the salts present in the three walls.

The use of ECOS/RUNSALT enable to set an interval of relative humidity where the risk of degradation caused by salt weathering is very high. Consequently, during the recovery phase, as drying occurs, when humidity falls within this range, the site manager will be alerted to the elevated risk of salt crystallisation, which could potentially lead to damage.

Conclusion

During the CHrisis project following the floods that affected Wallonia in 2021, the monument laboratory studied eight heritage buildings. In this study, two models, Sedlbauer's isopleths and ECOS/RUNSALT were evaluated to predict the risk of mould and salt weathering, respectively.

The risk assessment carried out with Sedlbauer's isopleths has been compared to the mould growth activity measured indirectly by the ATP meter. An acceptable level of agreement was found, but future research could enhance it by calculating the millimetres of mould growth as a function of time (over the different periods) and comparing it with the 'signal light' rule from WUFI–Bio.[23] This rule defines the mould risk based on annual mould growth.

In all cases, the growth activities were consistent with Sedlbauer's isopleths and the periods at risk for mould growth have been identified. Consequently, the person responsible for the site during the drying process in the recovery phase can focus on actions such as ventilation or other treatments only during these 'at–risk' periods.

The ECOS/RUNSALT model facilitated the prediction of the relative humidity range during which the salts in building may lead to damage. This range is associated with an increased risk during the building's drying process after flooding and requires greater attention.

Consequently, site managers will utilise both models during the recovery phase to prioritise actions and prevent secondary damage related to salt weathering and mould growth.

During the recovery phase, the site manager must monitor climatic conditions at the affected site. By employing this data in the Seldbauer isopleth model, the site manager can ascertain whether there is a high risk of mould growth. In the case of Trooz, a metal grille was constructed and positioned over the main entrance to prevent any unauthorised access to the church when the door was open. When a high–risk period was identified by this model, the door was opened wide, as were the sacristy windows and high openings in the nave, to create natural cross–ventilation and reduce climatic conditions to a lower risk of biological development.

With regard to the risk of salt weathering, the results from the wall samples have provided insights into the humidity range that promotes salt crystallisation and may lead to degradation. Given that this range is fairly wide, it is advisable to keep evaporation slow and relative humidity fairly high, trying not to over–ventilate only when a high risk of mold growth is identified. If heating is possible a temperature not higher than 15°C should be achieved. This was not possible at Trooz.

Appendix 1

This appendix compiles the crystallisation behaviour obtained from thermodynamic calculations conducted with ECOS/RUNSALT.

West wall of the nave – Plaster, 20cm: 1.86%

[Fig. 11]

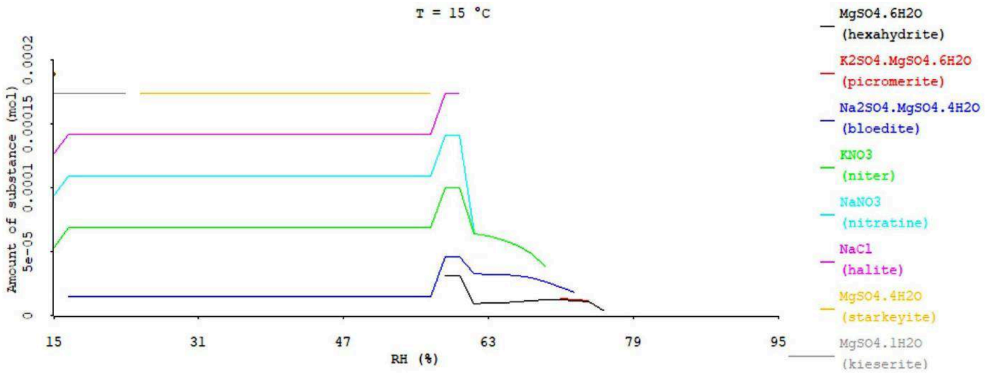

Crystallisation behaviour at variable relative humidity (15–95%) with a resolution of 0.2% (x–axis) and temperature at 15°C of the ion mixture detected in a joint mortar sample (after the subtraction of an equimolar content of sodium, calcium, and sulphate ions) generated by the ECOS–RUNSALT model. The relative amount of substance is expressed as a fraction of crystalline salt (n/n_{tot}) y–axis.

West wall of the nave – Mortar, surface, 20cm: 1.16%

[Fig. 12]

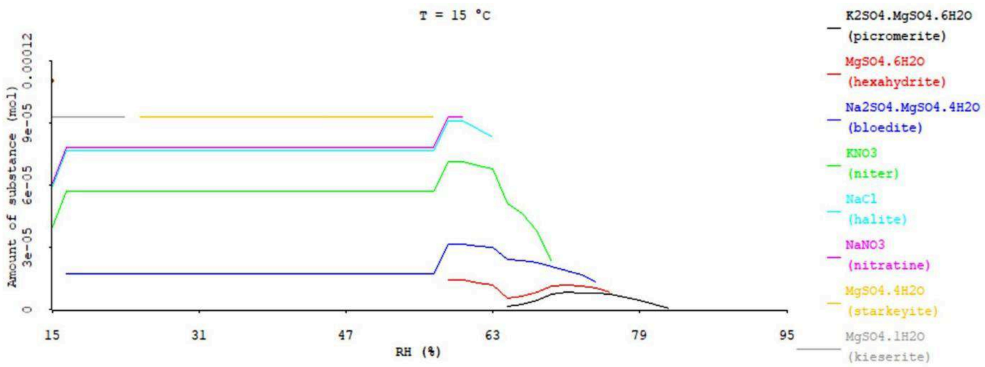

Crystallisation behaviour under varying relative humidity (15–95%) with a resolution of 0.2% (x–axis) at 20°C and 15°C for the mixture of ions identified in a joint mortar sample (after subtracting an equimolar content of sodium, calcium, and sulphate ions) produced by the ECOS– RUNSALT model. The relative amount of substance is expressed as a fraction of crystalline salt (n/n_{tot}) (y–axis).

West wall of the nave – Plaster, 50cm: 2.03%

[Fig. 13]

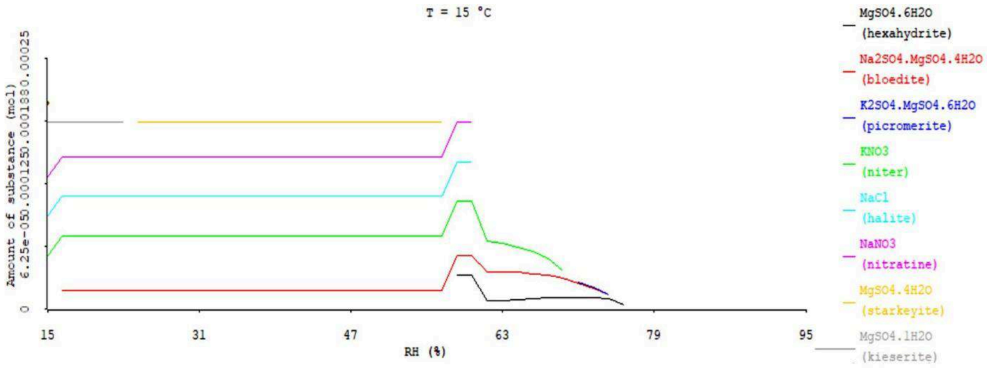

Crystallisation behaviour under varying relative humidity (15–95%) with a resolution of 0.2% (x–axis) at 20°C and 15°C for the mixture of ions identified in a joint mortar sample (after subtracting an equimolar content of sodium, calcium, and sulphate ions) produced by the ECOS– RUNSALT model. The relative amount of substance is expressed as a fraction of crystalline salt (n/n_{tot}) (y–axis).

West wall of the nave – Mortar, surface, 50cm: 2.40%

[Fig. 14]

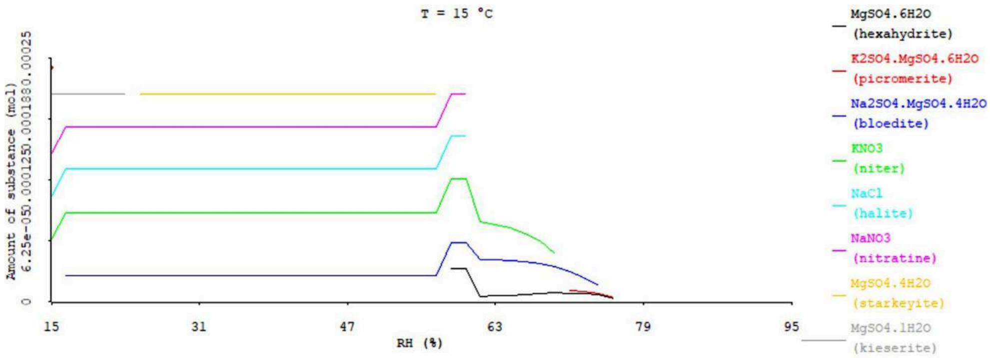

Crystallisation behaviour at variable relative humidity (15–95%) with a resolution of 0.2% (x–axis) at 20°C and 15°C, of the ionic mixture detected in a joint mortar sample (after subtracting an equimolar content of sodium, calcium, and sulphate ions) generated by the ECOS– RUNSALT model. The relative amount of substance is expressed as a fraction of crystalline salt (n/n_{tot}) (y–axis).

West wall of the nave – Mortar, depth, 50cm: 1.40%

[Fig. 15]

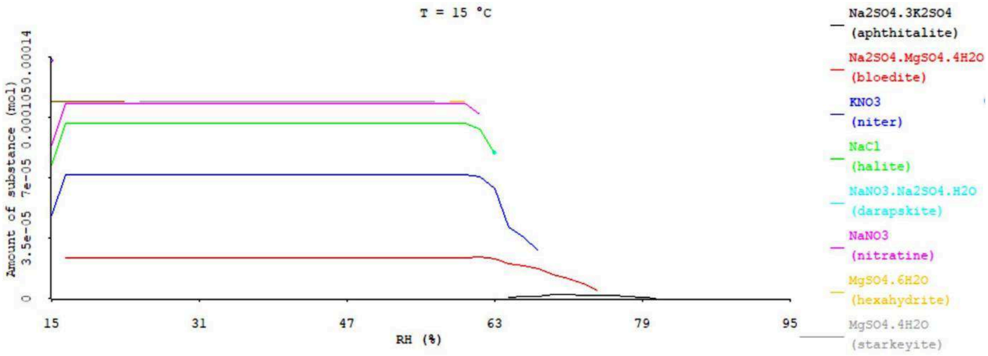

The crystallisation behaviour at varying relative humidity (15–95%) with a resolution of 0.2% (x–axis), and temperatures at 20°C (or 15°C), of the ion mixture detected in a joint mortar sample (after the subtraction of an equimolar content of sodium, calcium, and sulphate ions) was generated by the ECOS– RUNSALT model. The relative amount of substance is presented as a fraction of crystalline salt (n/n_{tot}) on the y–axis.

West wall of the nave – Plaster, 100cm: 1.55%

[Fig. 16]

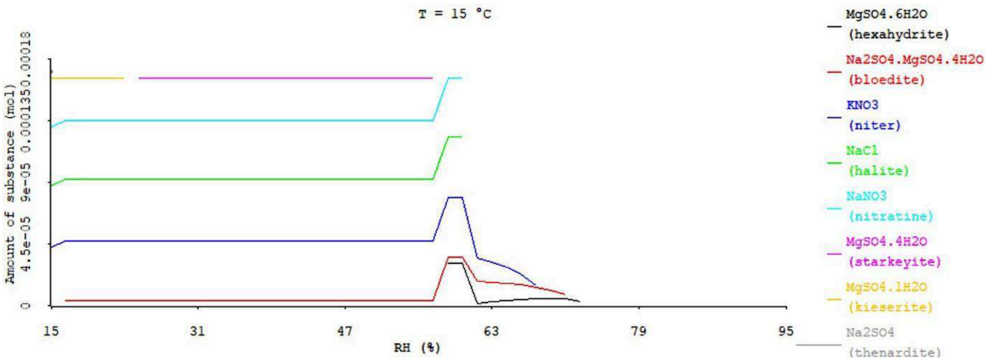

Crystallisation behaviour at varying relative humidity (15–95%) with a resolution of 0.2% (x–axis) and temperature maintained at 20°C (or 15°C) of the ion mixture detected in a joint mortar sample (after subtracting an equimolar content of sodium, calcium, and sulphate ions) generated by the ECOS–RUNSALT model. The relative amount of substance is expressed as a fraction of crystalline salt (n/n_{tot}) on the y–axis.

West wall of the nave – Mortar, surface, 100cm: 2.50%

[Fig. 17]

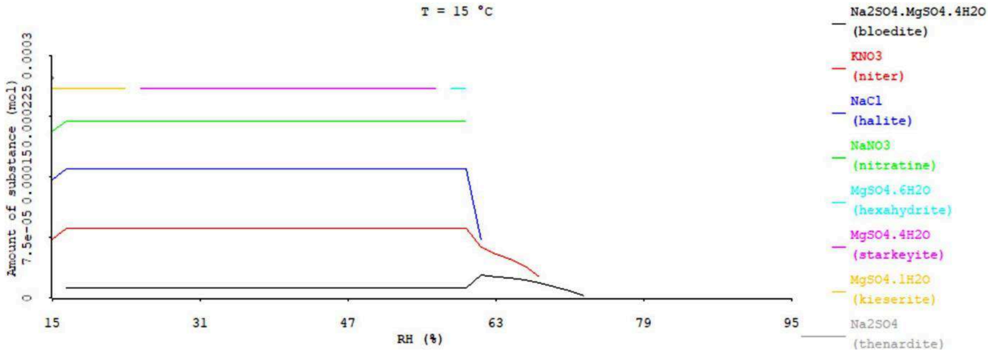

Crystallisation behaviour at varying relative humidity (15–95%) with a resolution of 0.2% (x–axis) and temperature maintained at 20°C (or 15°C) of the ion mixture detected in a joint mortar sample (after subtracting an equimolar content of sodium, calcium, and sulphate ions) generated by the ECOS–RUNSALT model. The relative amount of substance is expressed as a fraction of crystalline salt (n/n_{tot}) on the y–axis.

West wall of the nave – Mortar, depth, 100cm: 1.41%

[Fig. 18]

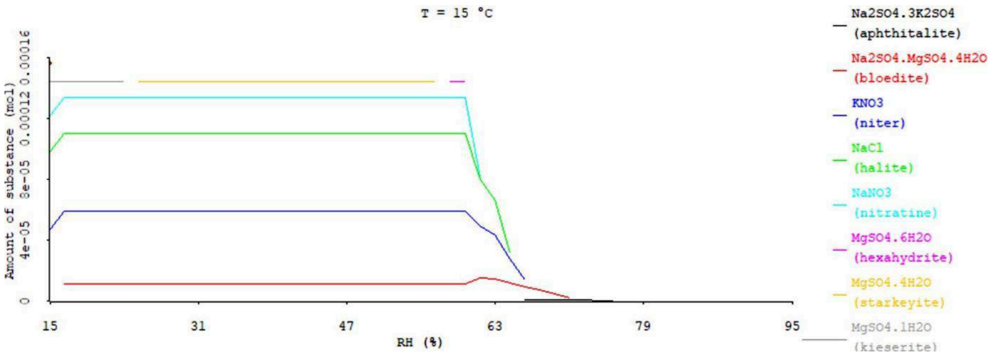

Crystallisation behaviour at varying relative humidity (15–95%) with a resolution of 0.2% (x–axis) and temperature maintained at 20°C (or 15°C) of the ion mixture detected in a joint mortar sample (after subtracting an equimolar content of sodium, calcium, and sulphate ions) generated by the ECOS–RUNSALT model. The relative amount of substance is expressed as a fraction of crystalline salt (n/n_{tot}) on the y–axis.

East wall of the nave – Plaster, 20 cm: 2.12%

[Fig. 19]

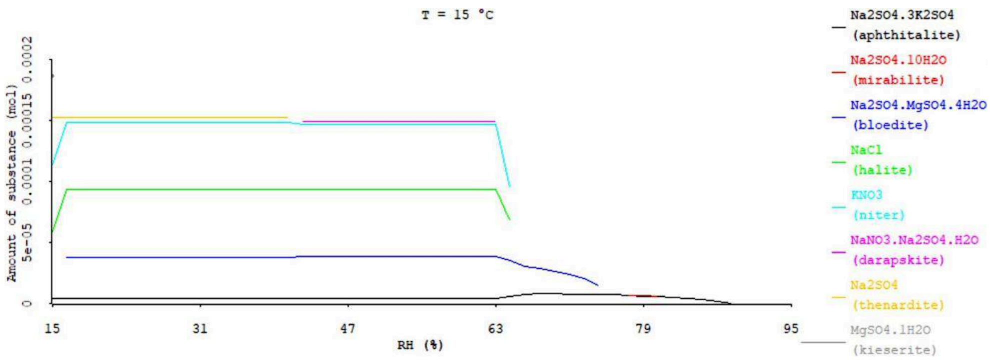

Crystallisation behaviour under varying relative humidity (15–95%) with a resolution of 0.2% (x–axis) at 20°C and 15°C for the mixture of ions identified in a joint mortar sample (after subtracting an equimolar content of sodium, calcium, and sulphate ions) produced by the ECOS– RUNSALT model. The relative amount of substance is expressed as a fraction of crystalline salt (n/n_{tot}) (y–axis).

East wall of the nave – Mortar, surface, 20cm: 1.85%

[Fig. 20]

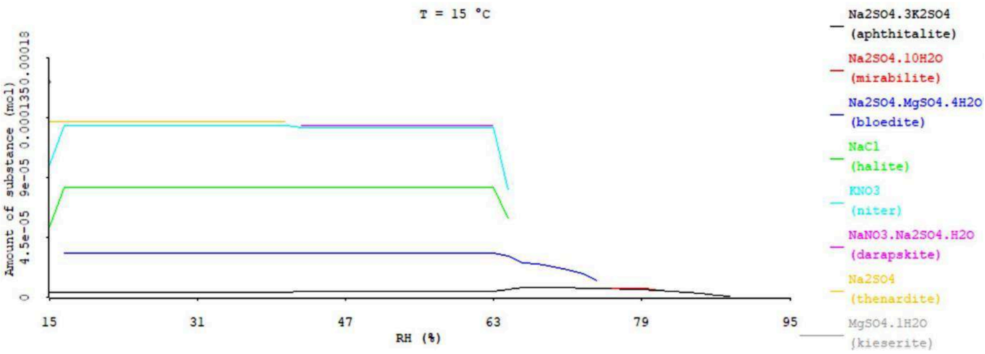

The crystallisation behaviour at varying relative humidity (15–95%) with a resolution of 0.2% (x–axis), and temperatures at 20°C (or 15°C), of the ion mixture detected in a joint mortar sample (after the subtraction of an equimolar content of sodium, calcium, and sulphate ions) was generated by the ECOS– RUNSALT model. The relative amount of substance is presented as a fraction of crystalline salt (n/n_{tot}) on the y–axis.

East wall of the nave – Plaster, 50cm: 2.16%

[Fig. 21]

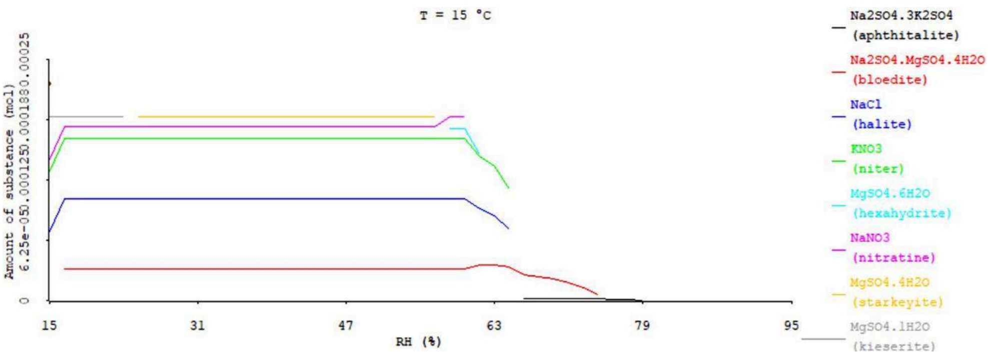

The crystallisation behaviour at varying relative humidity (15–95%) with a resolution of 0.2% (x–axis) and temperatures of 20°C (or 15°C) for the ion mixture detected in a joint mortar sample (after subtracting an equimolar content of sodium, calcium, and sulphate ions) was generated by the ECOS–RUNSALT model. The relative amount of substance is presented as a fraction of crystalline salt (n/n_{tot}) on the y–axis.

East wall of the nave – Mortar, surface, 50cm: 1.36%

[Fig. 22]

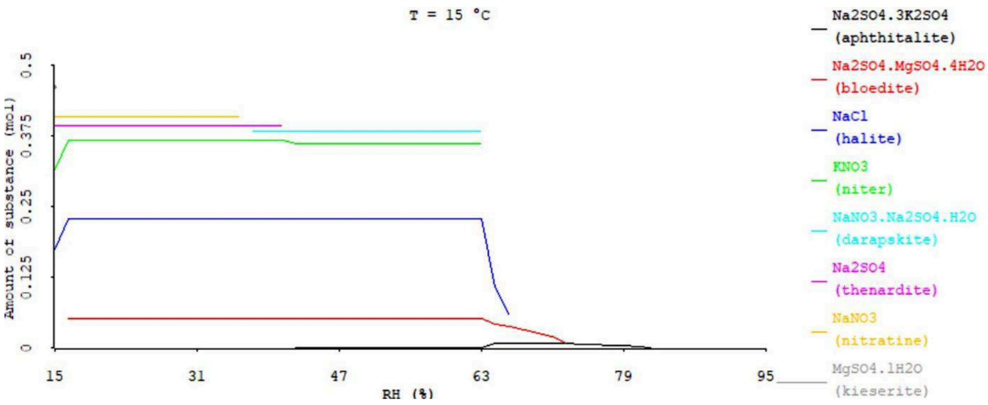

Crystallisation behaviour at varying relative humidity (15–95%) with a resolution of 0.2% (x–axis) and temperature maintained at 20°C (or 15°C) of the ion mixture detected in a joint mortar sample (after subtracting an equimolar content of sodium, calcium, and sulphate ions) generated by the ECOS–RUNSALT model. The relative amount of substance is expressed as a fraction of crystalline salt (n/n_{tot}) on the y–axis.

East wall of the nave – Mortar, Depth, 50cm: 1.06%

[Fig. 23]

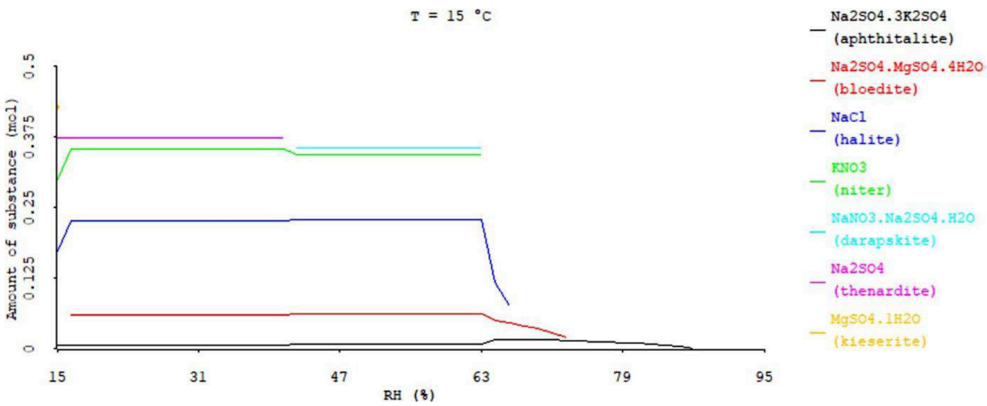

The crystallisation behaviour at varying relative humidity (15–95%) with a resolution of 0.2% (x–axis), and temperatures at 20°C (or 15°C), of the ion mixture detected in a joint mortar sample (after the subtraction of an equimolar content of sodium, calcium, and sulphate ions) was generated by the ECOS– RUNSALT model. The relative amount of substance is presented as a fraction of crystalline salt (n/n_{tot}) on the y–axis.

East wall of the nave – Plaster, 100cm: 1.21%

[Fig. 24]

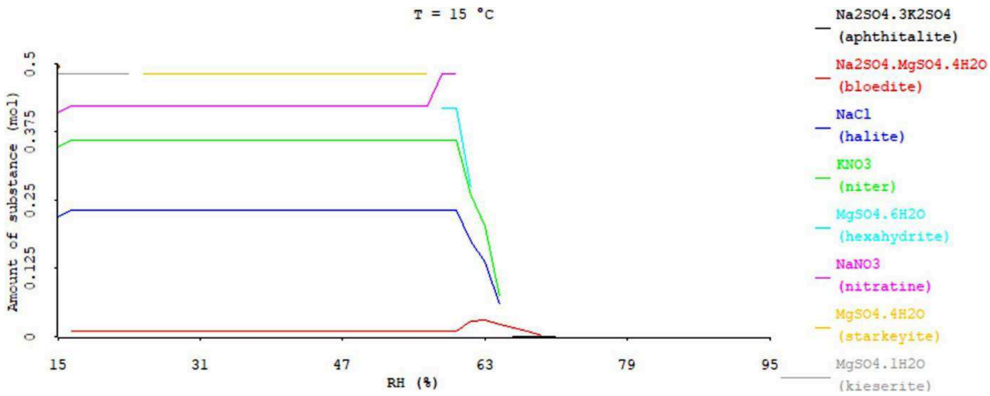

Crystallisation behaviour under varying relative humidity (15–95%) with a resolution of 0.2% (x–axis) at 20°C and 15°C for the mixture of ions identified in a joint mortar sample (after subtracting an equimolar content of sodium, calcium, and sulphate ions) produced by the ECOS– RUNSALT model. The relative amount of substance is expressed as a fraction of crystalline salt (n/n_{tot}) (y–axis).

East wall of the nave – Mortar, surface 100cm: 1.51%

[Fig. 25]

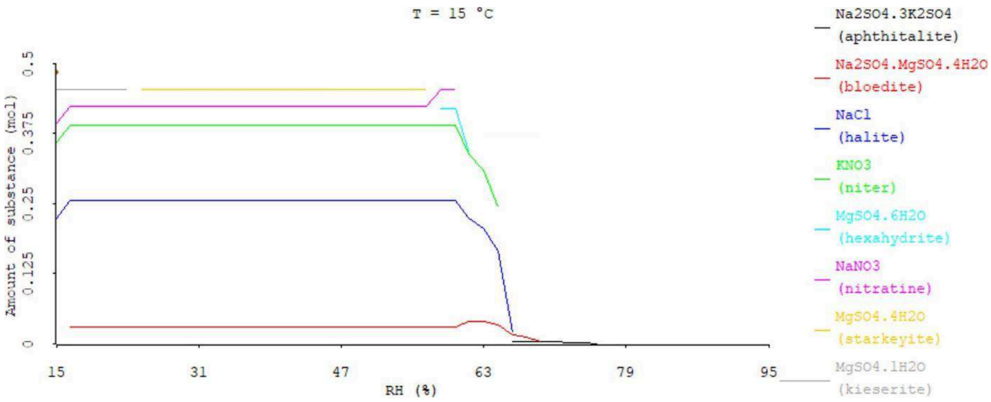

The crystallisation behaviour at varying relative humidity (15–95%) with a resolution of 0.2% (x–axis), and temperatures at 20°C (or 15°C), of the ion mixture detected in a joint mortar sample (after the subtraction of an equimolar content of sodium, calcium, and sulphate ions) was generated by the ECOS– RUNSALT model. The relative amount of substance is presented as a fraction of crystalline salt (n/n_{tot}) on the y–axis.

East wall of the nave – Mortar, Depth, 150 cm: 1.27%

[Fig. 26]

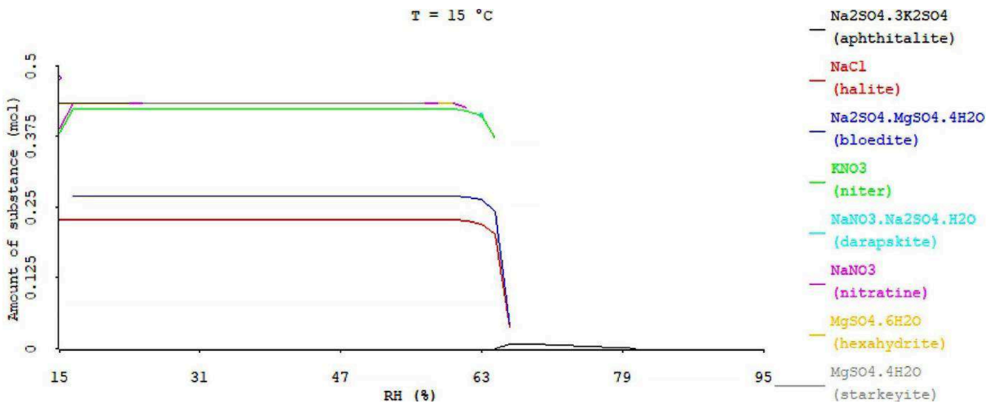

The crystallisation behaviour at varying relative humidity (15–95%) with a resolution of 0.2% (x–axis), and temperatures at 20°C (or 15°C), of the ion mixture detected in a joint mortar sample (after the subtraction of an equimolar content of sodium, calcium, and sulphate ions) was generated by the ECOS– RUNSALT model. The relative amount of substance is presented as a fraction of crystalline salt (n/n_{tot}) on the y–axis.

BIBLIOGRAPHY

Ali *et al.* 2020 A.A. Ali, A.B. Altemimi, N. Alhelfi and S.A. Ibrahim, *Application of Biosensors for Detection of Pathogenic Food Bacteria: A Review*, in *Biosensors* (Basel), 10, 6 (https://doi.org/10.3390/bios10060058), 2020, p. 58.

Ayerst 1969 G. Ayerst, *The effect of moisture and temperature on growth and spore germination in some fungi*, in *Journal of Stored Products Research*, 5 (https://doi.org/10.1016/0022-474X(69)90055-1), 1969, p. 127-141.

Birkmann *et al.* 2010 J. Birkmann, P. Buckle, J. Jaeger, M. Pelling, N. Setiadi, M. Garschagen, N. Fernando and J. Kropp, *Extreme events and disasters: a window of opportunity for change? Analysis of organizational, institutional and political changes, formal and informal responses after mega–disasters*, in *Natural Hazards*, 55, 2010, p. 637-655.

Blades and Skipper 2023 N. Blades and P. Skipper, *Classification obtained from the webinar Icon Care of Collections Group AGM* – Mould (webinar, 26 April 2023) (https://www.icon.org.uk/events/care–of–collections–group–2023–agm–mould.html), 2023.

Clarke *et al.* 1999 J. Clarke, C. Johnstone, N. Kelly, R. McLean, J. Anderson, N. Rowan and J.E. Smith, *A technique for the prediction of the conditions leading to mould growth in buildings*, in *Build and Environment*, 34 (https://doi.org/10.1016/S0360-1323(98)00023-7), 1999, p. 515-521.

Clegg and Brimblecombe 2000 S.L. Clegg and P. Brimblecombe, *Pitzer model of electrolyte solutions*, in C. Price, *An expert chemical model for determining the environmental conditions needed to prevent salt damage in porous materials, Project ENV4–CT95–0135 (1996–2000)* (https://predict.kikirpa.be/wp–content/uploads/2022/01/Price–2000–An–expert–chemical–model–for–determining–the–envir.pdf), London, 2000, p. 13-18.

Eeckout 2014 L. Eeckout, *L'humidité dans les constructions. Particularités de l'humidité ascensionnelle*, in *Note d'information technique 252 – CSTC* (https://www.biu.pt/media/products/documents/2014–cstc–nit–252.pdf), 2014, p. 22.

Eng Moore and Maitland 2024 T. Eng Moore and C. Maitland, *How do we assess mould levels? Testing the parameters of rapid adenosine bioluminescent swabs in conservation*, in *Journal of the Institute of Conservation*, 47, 1 (https://doi.org/10.1080/19455224.2023.2299449), 2024, p. 3-21.

Godts *et al.* 2022 S. Godts, M. Steiger, S.A. Orr, T. De Kock, J. Desarnaud, H. De Clercq and V. Cnudde, *Charge balance calculations for mixed salt systems applied to a large dataset from the built environment*, in *Scientific Data*, 9, 324 (https://doi.org/10.1038/s41597–022–01445–9), 2022.

Hawkesbury–Nepean Floodplain Management Steering Committee 2006 Hawkesbury–Nepean Floodplain Management Steering Committee, *Reducing vulnerability of buildings to flood damage: guidance on building in flood prone areas* (https://www.ses.nsw.gov.au/sites/default/files/2024–02/building_guidelines.pdf), Parramatta, 2006.

Hens 1990 H. Hens, *Condensation and Energy: Guidelines and Practices*, in *IEA–Exco ECBCS* 2 (https://www.iea–ebc.org/Data/publications/EBC_Appendix_14_guidelines_and_practice.pdf), Leuven, 1990.

Kreienkamp *et al.* 2021 F. Kreienkamp, Y.P. Sjoukje, J.S. Tradowsky, S.F. Kew, P. Lorenz, J. Arrighi, A. Belleflamme, T. Bettmann, S. Caluwaerts, S.C. Chan, C.A. Ciavarella, L. De Cruz, H. de Vries, N. Demuth, A. Ferrone, M. Fischer, H.J. Fowler, K. Goergen, D. Heinrich, Y. Henrichs, G. Lenderink, F. Kaspar, E. Nilson, F.E.L. Otto, F. Ragone, S.I. Seneviratne, R.K. Singh, A. Skålevåg, P. Termonia, L. Thalheimer, M. van Aalst, J. Van den Bergh, H. Van de Vyver, S. Vannitsem, G.J. van Oldenborgh, B. Van Schaeybroeck, R. Vautard, D. Vonk and N. Wanders, *Rapid attribution of heavy rainfall events leading to the severe flooding in Western Europe during July 2021*, in *World Weather Attribution* (https://www.worldweatherattribution.org/wp-content/uploads/Scientific-report-Western-Europe-floods-2021-attribution.pdf), 2021.

Leissner *et al.* 2015 J. Leissner, R. Kilian, L. Kotova, D. Jacob, U. Mikolajewicz, T. Broström, J. Ashley–Smith, H. Schellen, M. Martens, J. Van Schijndel, F. Antretter, M. Winkler, C. Bertolin, D. Camuffo, G. Simeunovic and T. Vyhlidal, *Climate for Culture: Assessing the impact of climate change on the future indoor climate in historic buildings using simulations*, in *Heritage Science*, 3 (https://www.researchgate.net/publication/286765723_Climate_for_Culture_assessing_the_impact_of_climate_change_on_the_future_indoor_climate_in_historic_buildings_using
2015, p. 38-52.

Mildenhall and Rankin 2020 K.B. Mildenhall and S.A. Rankin, *Implications of adenylate metabolism in hygiene assessment: A review*, in *Journal of Food Protection*, 83 (https://pubmed.ncbi.nlm.nih.gov/32338738/), 2020, p. 1619-1631.

Pasanen *et al.* 2000 A.–L. Pasanen, J.P. Kasanen, S. Rautiala, M. Ikäheimo , J. Rantamäki, H. Kääriäinen and P. Kalliokoski, *Fungal Growth and Survival in Building Materials under Fluctuating Moisture and Temperature Conditions*, in *International Biodeterioration and Biodegradation*, 46, 2, 2000, p. 117-127.

Pickels *et al.* 2015 D. Pickels, P. Rhodes, J. Gooch, J. Garlick, N. Kelly, P. Hadley and S. Berry, *Flooding and historic building*, London, 2015.

Price 2000 C. Price, *An expert chemical model for determining the environmental conditions needed to prevent salt damage in porous materials: protection and conservation of the European cultural heritage, project ENV4–CT95–0135 (1996–2000)* (European Commission. *Technologies to Protect and Rehabilitate*

European Cultural Heritage) (https://predict.kikirpa.be/wp–content/uploads/2022/01/Price–2000–An–expert–chemical–model–for–determining–the–envir.pdf), London, 2000.

Rowan *et al.* 1999 N. Rowan, C. Johnstone, R. Craig, J. Anderson and J. Clarke, *Prediction of toxigenic fungal growth in buildings by using a novel modelling system*, in *Applied and Environmental Microbiology*, 65 (https://pubmed.ncbi.nlm.nih.gov/10543791/), 1999, p. 4814-4821.

Schoenmaeckers and Blistein 2024 C. Schoenmaeckers and H. Blistein, *Patrimoine architectural et sites classés en Province de Liège: impact des inondations et constats actuels*, *Autour des premiers soins au Patrimoine* (study day, Liège, City of Liège, 6 June 2024), 2024.

Sedlbauer 2001 K. Sedlbauer, *Vorhersage von Schimmelpilzbildung auf und in Bauteilen*, PhD thesis in Civil Engineering, Universität Stuttgart (https://www.ibp.fraunhofer.de/content/dam/ibp/ibp-neu/de/dokumente/dissertationen/ks_dissertation_tcm45–30724.pdf), 2001.

Sedlbauer 2002 K. Sedlbauer, *Prediction of Mould Growth by Hygrothermal Calculation*, in *Journal of Building Physics*, 25 (https://www.researchgate.net/publication/238185805_Prediction_of_Mould_Growth_by_Hygrothermal_Calculation), 2002, p. 321-336.

Smith and Hill 1982 S. Smith and S.T. Hill, *Influence of temperature and water activity on germination and growth of Aspergillus restrictus and A. versicolor*, in *Transactions of the British Mycological Society*, 79 (https://www.sciencedirect.com/science/article/abs/pii/S0007153682800582?via%3Dihub), 1982, p. 558-560.

Tandon 2018 A. Tandon, *First aid to cultural heritage in times of crisis*, in *ICCROM – Centre for the Study of the Preservation and Restoration of Cultural Property* (https://www.iccrom.org/sites/default/files/2018–10/fac_handbook_print_oct-2018_final.pdf), 2018.

Vereecken, Vanoirbeek and Roels 2015 E. Vereecken, K. Vanoirbeek and S. Roels, *Towards a more thoughtful use of mould prediction models: A critical view on experimental mould growth research*, in *Journal of Building Physics*, 39 (https://doi.org/10.1177/1744259115588718), 2015, p. 102-123.

NOTES

1. Leissner *et al.* 2015.
2. Hawkesbury–Nepean Floodplain Management Steering Committee 2006.
3. Pickels *et al.* 2015.
4. Birkmann *et al.* 2010; Tandon 2018.
5. Pickels *et al.* 2015.
6. Kreienkamp *et al.* 2021.
7. Schoenmaeckers and Blistein 2024.
8. Birkmann *et al.* 2010.
9. Eeckout 2014, p. 22.
10. Godts *et al.* 2022.
11. Price 2000.
12. Clegg and Brimblecombe 2000.
13. Ayerst 1969.
14. Smith and Hill 1982.
15. Hens 1990; Clarke *et al.* 1999.
16. Sedlbauer 2001.
17. Sedlbauer 2002.
18. Ali *et al.* 2020.
19. Mildenhall and Rankin 2020.

20. Eng Moore and Maitland 2024.
21. Blades and Skipper 2023.
22. Pasanen *et al.* 2000.
23. Vereecken, Vanoirbeek and Roels 2015.

ABSTRACTS

Built heritage represents a non–renewable resource that remains fragile and highly vulnerable to climate change. Climate change goes hand–in–hand with extreme weather events, including droughts, floods, severe storms, and prolonged heatwaves.
In July 2021, the Walloon region of Belgium experienced severe flooding, impacting over 10% of the heritage buildings in the Liège province. This paper evaluates the application of two predictive models, Sedlbauer's isopleths and ECOS/RUNSALT, during the post–flood recovery phase in Wallonia. These models aim to mitigate secondary damages associated with salt weathering and mould growth. The findings underscore the models' usefulness for site managers in prioritising intervention strategies, thus reducing the risk of further deterioration and ensuring a more targeted and efficient recovery process.

Le patrimoine bâti constitue un héritage culturel irremplaçable, particulièrement vulnérable aux impacts du changement climatique. Ce dernier s'accompagne d'une intensification des phénomènes météorologiques extrêmes tels que les sécheresses, les inondations, les tempêtes intenses ou encore les vagues de chaleur prolongées.
En juillet 2021, la région wallonne de Belgique a été confrontée à des inondations d'une ampleur exceptionnelle, affectant plus de 10 % des édifices patrimoniaux de la province de Liège. Cette étude s'intéresse à l'intégration de deux modèles prédictifs – les isoplèthes de Sedlbauer et le modèle ECOS/RUNSALT – dans le cadre de la phase de reconstruction post–inondation en Wallonie. Ces outils ont pour objectif d'anticiper les dommages secondaires, en particulier ceux liés à l'altération saline et à la prolifération de moisissures. Les résultats mettent en évidence la pertinence de ces modèles pour les gestionnaires de sites patrimoniaux, leur permettant d'établir des priorités d'intervention, de réduire les risques de dégradation supplémentaire et de favoriser une stratégie de restauration plus ciblée et efficace.

Onroerend erfgoed is onvervangbaar en uiterst kwetsbaar voor klimaatverandering. Klimaatverandering gaat hand in hand met extreme weersomstandigheden, waaronder droogtes, overstromingen, zware stormen en langdurige hittegolven.
In juli 2021 kreeg het Waalse Gewest van België te maken met een verwoestende overstroming die meer dan 10% van het bouwkundige erfgoed in de provincie Luik trof. Dit artikel evalueert de toepassing van twee voorspellende modellen, de isopleten van Sedlbauer en ECOS/RUNSALT, tijdens de herstelfase na de overstroming in Wallonië. Deze modellen zijn bedoeld om secundaire schade, met name door zoutverwering en schimmelgroei, te beperken. De bevindingen onderstrepen het nut van de modellen voor sitebeheerders bij het prioriteren van interventiestrategieën om het risico op verdere degradatie te verkleinen en een gerichter en efficiënter herstelproces te garanderen.

INDEX

Mots-clés: reconstruction, inondations, prévision, prolifération des moisissures, altération saline
Trefwoorden herstel, overstroming, voorspelling, schimmelgroei, zoutverwering
Keywords: recovery, Floods, Prediction, mould growth, salt weathering

AUTHORS

JOSÉ VETRO

José Vetro is a conservator–restorer of wall and easel paintings. He completed his master's studies in Art Conservation–Restoration, specialising in painting, at École Supérieure des Arts (ESA) Saint–Luc Liège in 2012. He subsequently participated in several mural painting restoration projects, working with Altritempi nv in 2013 and 2016, and with SRAL (Stichting Restauratie Atelier Limburg) from 2014 to 2015 and again from 2020 to 2022. From 2017 to 2021, he collaborated on various mural and easel painting restoration projects with Artbee srl. Since 2022, he has been part of the Royal Institute for Cultural Heritage (KIK–IRPA) in the Laboratory of Monuments.

JULIE DESARNAUD

Dr. Julie Desarnaud is a physical chemist specialising in the study of building materials. After completing her Ph.D. on the degradation of porous media due to salt crystallisation, she pursued a postdoctoral fellowship at the Laboratoire Navier, focusing on the durability and conservation of construction materials in Paris. Subsequently, she worked as a researcher at the Institute of Physics at the University of Amsterdam, concentrating her research on damage to building stone and the effects of climate change. Following a two–year tenure at the Getty Conservation Institute, where she served as a scientist on the Built Heritage Research Initiative, she joined the Royal Institute for Cultural Heritage (KIK–IRPA) in 2020 in the Laboratory of Monuments.